

Integrin binding specificity regulates biomaterial surface chemistry effects on cell differentiation

Benjamin G. Keselowsky^{*†}, David M. Collard[‡], and Andrés J. García^{*†§}

^{*}Woodruff School of Mechanical Engineering, [†]Petit Institute for Bioengineering and Bioscience, and [‡]School of Chemistry and Biochemistry, Georgia Institute of Technology, Atlanta, GA 30332

Edited by Sheldon Weinbaum, City College of the City University of New York, New York, NY, and approved March 17, 2005 (received for review October 4, 2004)

Biomaterial surface chemistry has profound consequences on cellular and host responses, but the underlying molecular mechanisms remain poorly understood. Using self-assembled monolayers as model biomaterial surfaces presenting well defined chemistries, we demonstrate that surface chemistry modulates osteoblastic differentiation and matrix mineralization independently from alterations in cell proliferation. Surfaces were precoated with equal densities of fibronectin (FN), and surface chemistry modulated FN structure to alter integrin adhesion receptor binding. OH- and NH₂-terminated surfaces up-regulated osteoblast-specific gene expression, alkaline phosphatase enzymatic activity, and matrix mineralization compared with surfaces presenting COOH and CH₃ groups. These surface chemistry-dependent differences in cell differentiation were controlled by binding of specific integrins to adsorbed FN. Function-perturbing antibodies against the central cell binding domain of FN completely inhibited matrix mineralization. Furthermore, blocking antibodies against β_1 integrin inhibited matrix mineralization on the OH and NH₂ surfaces, whereas function-perturbing antibodies specific for β_3 integrin increased mineralization on the COOH substrate. These results establish surface-dependent differences in integrin binding as a mechanism regulating differential cellular responses to biomaterial surfaces. This mechanism could be exploited to engineer materials that control integrin binding specificity to elicit desired cellular activities to enhance the integration of biomaterials and improve the performance of biotechnological culture supports.

cell adhesion | signaling | osteoblast | mineralization

Biomaterial surface chemistry modulates *in vitro* and *in vivo* cellular responses, including adhesion, survival, cell cycle progression, and expression of differentiated phenotypes (1–8). These cell-material interactions regulate cell and host responses to implanted devices, biological integration of biomaterials and tissue-engineered constructs, and the performance of cell arrays and biotechnological cell culture supports (9–12). For instance, anionic and neutral hydrophilic surfaces increase macrophage/monocyte apoptosis and reduce macrophage fusion to modulate inflammatory responses to implanted materials (8). The effects of biomaterial surface properties on cellular responses are generally attributed to material-dependent differences in adsorbed protein species, concentration, and/or biological activity. Nonetheless, the molecular mechanisms modulating these substrate-dependent, complex higher-order cellular activities remain poorly understood. This lack of a fundamental understanding of cell-material interactions hinders progress toward the development of synthetic materials that elicit desired cellular responses. Using self-assembled monolayers (SAMs) presenting well defined chemistries as model biomaterial surfaces, we previously showed that surface chemistry modulates the structure and activity of adsorbed fibronectin (FN) (13). These differences in FN structure alter integrin receptor binding, resulting in selective binding of $\alpha_5\beta_1$ integrin on OH and NH₂ surfaces, binding of both $\alpha_5\beta_1$ and $\alpha_V\beta_3$ on the COOH surface, and poor binding of either integrin on the CH₃ SAM (13, 14).

These surface chemistry-dependent differences in integrin binding differentially regulate focal adhesion composition and signaling (14). In the present work, we demonstrate that integrin binding specificity for adsorbed FN regulates the differential effects of biomaterial surface chemistry on osteoblast differentiation and mineralization. These findings establish a mechanism for the diverse cellular responses elicited by synthetic materials and provide design principles for the engineering of biomaterials that direct cell function.

Materials and Methods

Cells and Antibodies. Human plasma FN and cell culture reagents were obtained from Invitrogen. FBS was purchased from HyClone, and BSA and chemical reagents were obtained from Sigma. Anti-BrdUrd (B44) and anti-human FN (HFN7.1) monoclonal antibodies were purchased from BD Immunocytometry and Developmental Studies Hybridoma Bank (Iowa City, IA), respectively. Function-blocking monoclonal antibodies directed against β_1 (Ha2/5) and β_3 (2C9.G2) integrin subunits and isotype controls were purchased from BD Pharmingen. Alexa Fluor 488-conjugated antibodies and ethidium homodimer 2 were purchased from Molecular Probes. The immature osteoblast-like cell line MC3T3-E1 was obtained from the RIKEN Cell Bank (Tokyo). Cells were maintained in α -MEM supplemented with 10% FBS and 1% penicillin-streptomycin and passaged every 2 days by using standard techniques. For all experiments, cells were seeded at 100 cells per mm² on FN-coated substrates in serum-containing media and cultured in growth media supplemented with 50 μ g/ml ascorbic acid and 2.1 mM Na- β -glycerophosphate to promote differentiation.

Model Biomaterial Surfaces. SAMs of alkanethiols on gold were used to present ordered surfaces with well defined chemistries. 1-dodecanethiol [HS-(CH₂)₁₁-CH₃], 11-mercapto-1-undecanol [HS-(CH₂)₁₁-OH], and 11-mercaptoundecanoic acid [HS-(CH₂)₁₀-COOH] were purchased from Aldrich, and 12-amino-1-mercaptododecane [HS-(CH₂)₁₂-NH₂] was synthesized in-house (13). SAMs of their respective alkanethiols are referred to hereafter as CH₃, OH, COOH, and NH₂ SAMs. Gold-coated culture plates were prepared by sequential deposition of titanium (100 Å) and gold (200 Å) films via an electron beam evaporator (2×10^{-6} Torr, 2 Å/s). SAMs were assembled by immersing gold-coated substrates in ethanolic alkanethiol solutions (1.0 mM) and characterized by contact angle goniometry and x-ray photoelectron spectroscopy. After rinsing in ethanol and equilibrating in Dulbecco's PBS (DPBS) for 15 min, SAMs were coated with FN diluted in DPBS for 30 min

This paper was submitted directly (Track II) to the PNAS office.

Abbreviations: ALP, alkaline phosphatase; FTIR, Fourier transform infrared; FN, fibronectin; SAM, self-assembled monolayer.

[§]To whom correspondence should be addressed at: Woodruff School of Mechanical Engineering, Georgia Institute of Technology, 315 Ferst Drive, Room 2314 IBB, Atlanta, GA 30332-0363. E-mail: andres.garcia@me.gatech.edu.

© 2005 by The National Academy of Sciences of the USA

and subsequently blocked for 30 min in 1% heat-denatured BSA to produce equal FN surface densities among SAMs (40 ng/cm²) (13).

Cell Proliferation and Gene Expression. BrdUrd (3.1 μg/ml) was added to cultures at 16 h postseeding and incubated for 4 h. After washing with DPBS, cultures were fixed in ice-cold 70% ethanol for 10 min and denatured in 4 M HCl for 20 min. After washing in DPBS and blocking in 5% FBS plus 1% serum albumin, cultures were incubated in anti-BrdUrd and Alexa Fluor 488-conjugated anti-mouse IgG antibodies. Cell nuclei were counterstained with ethidium homodimer 2. Cultures were scored by fluorescence microscopy for proliferation as the percentage of cells positive for BrdUrd incorporation relative to cell nuclei.

Osteoblast-specific gene expression was analyzed at day 7 by real-time PCR (15). Total RNA was isolated by using Qiagen RNEasy kits, and cDNA synthesis was performed on DNase I-treated (25 Kunitz units) total RNA (1 μg) by oligo(dT) priming with the SuperScript II preamplification system (Invitrogen). Real-time PCR with SYBR green intercalating dye and osteoblast-specific primers was performed with an Applied Biosystems ABI Prism 7700 (15). Standards for each gene were amplified from cDNA by using oligonucleotide primers, purified by using a Qiagen PCR purification kit, and diluted over a functional range of concentrations. Transcript concentration in template cDNA solutions was quantified from a linear standard curve, normalized to 1 μg of total RNA, and expressed as femtomoles of transcripts per microgram of total RNA.

Alkaline Phosphatase (ALP) Activity and Matrix Mineralization. ALP enzymatic activity was quantified biochemically (15). Cultures (14 day) were scraped into ice-cold 50 mM Tris·HCl, sonicated, and normalized for total protein. ALP activity was quantified by reaction in 5-methyl umbelliferyl phosphate substrate (60 μg/ml) in diethanolamine buffer (pH 9.5). The resulting fluorescence was measured at 360-nm excitation/465-nm emission, and ALP activity was calculated from a purified ALP standard. For mineralization analyses, 14-day cultures were fixed in 70% ethanol and von Kossa-stained (15). Plates were scored for percent mineralization by image analysis. The chemical composition of matrices was examined by Fourier transform infrared (FTIR) spectroscopy (15). For inhibition experiments, blocking antibodies (HFN7.1, 10 μg/ml; integrin subunit-specific antibodies, 100 μg/ml) or isotype controls (100 μg/ml) were added to culture media on day 1 for the remainder of culture.

Statistical Analyses. Results were analyzed by ANOVA in SYSTAT 8.0 (SPSS, Chicago). Pairwise comparisons were performed by using Tukey's post hoc test; a 95% confidence level was considered significant.

Results

Surface Chemistry Modulates Osteoblast Differentiation and Mineralization. Ordered, well packed SAMs of ω-functionalized alkanethiols were selected as model biomaterials to present four surface chemistries: (i) CH₃ (hydrophobic), (ii) OH (neutral hydrophilic), (iii) COOH (negatively charged at pH 7.4), and (iv) NH₂ (positively charged at pH 7.4). Before cell-seeding, surfaces were coated with a specified FN density and blocked with heat-denatured albumin to prevent adsorption of additional proteins from serum-containing media that may influence cell behaviors. This experimental model provides a well defined system with an initial single adhesive ligand. Using this system, we recently demonstrated that surface chemistry alters the functional presentation of the major integrin binding domain of adsorbed FN (13). These substrate-dependent differences in FN activity modulate integrin binding in MC3T3-E1 cells. Although these cells express several integrins, including α₂β₁, α₃β₁, α₄β₁,

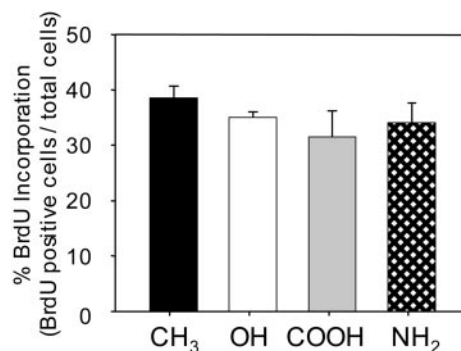


Fig. 1. Surface chemistry does not alter osteoblast proliferation. MC3T3-E1 cells were cultured on SAMs coated with equivalent FN surface densities (40 ng/cm²) for 16 h and pulsed with BrdUrd for 4 h before analysis.

α₅β₁, α₆β₁, α_vβ₁, and α_vβ₃, integrins α₅β₁ and α_vβ₃ are the major receptors for FN, as demonstrated by blocking with inhibitory antibodies. A fixed FN density (40 ng/cm²) was selected for cell proliferation and differentiation analyses. For this FN density (which is the saturation density for the OH SAM and lowest saturation density of all SAMs), the OH and NH₂ surfaces exhibit selective binding of α₅β₁ integrin, whereas the COOH SAM supports binding of both α₅β₁ and α_vβ₃, and the CH₃ surface poorly binds either integrin. Notably, function-perturbing antibodies directed against the central cell binding domain of human FN (which contains the RGD motif and binds to α₅β₁ and α_vβ₃) or integrin subunits completely block initial adhesion to these surfaces, demonstrating that the adsorbed FN, not proteins adsorbed from solution or deposited by the cells, provide the primary initial adhesion mechanism in this model (13).

MC3T3-E1 immature osteoblasts were selected to examine the effects of surface chemistry on cellular activities. Under appropriate culture conditions, this murine cell line up-regulates osteoblast-specific genes and produces mineralized nodules, undergoing the developmental stages associated with differentiating osteoblasts (16, 17). Furthermore, osteoblastic differentiation and matrix mineralization in this cell model are FN-dependent (18). Cells were seeded on FN-coated surfaces in serum-containing media, and no differences were observed in initial adherent numbers. Analysis of cell proliferation by BrdUrd incorporation revealed no differences among surface chemistries (Fig. 1). Total DNA measurements confirmed these observations.

To investigate the effects of surface chemistry on osteoblastic differentiation, bone-specific gene expression was quantified via real-time RT-PCR. ALP is an osteoblastic metabolic enzyme involved in mineral deposition and is an early marker of osteoblastic differentiation (19). Bone sialoprotein (BSP) is a matrix molecule deposited by osteoblasts that is responsible for mineralized nodule nucleation, and osteocalcin (OCN) is an extracellular matrix protein and a common marker of mature osteoblasts (19). Both early (ALP) and late (BSP and OCN) markers of osteoblastic differentiation exhibited elevated gene expression levels on the OH and NH₂ surfaces compared with the COOH and CH₃ SAMs (Fig. 2). In agreement with cell proliferation and number data, no differences in expression levels for the housekeeping gene β-actin were observed among surface chemistries. These results demonstrate surface chemistry-dependent differences in osteoblastic gene expression. Furthermore, the effects of surface chemistry on gene expression were specific to the osteoblast differentiation program and independent from alterations in cell proliferation.

The functional consequences of these surface chemistry-

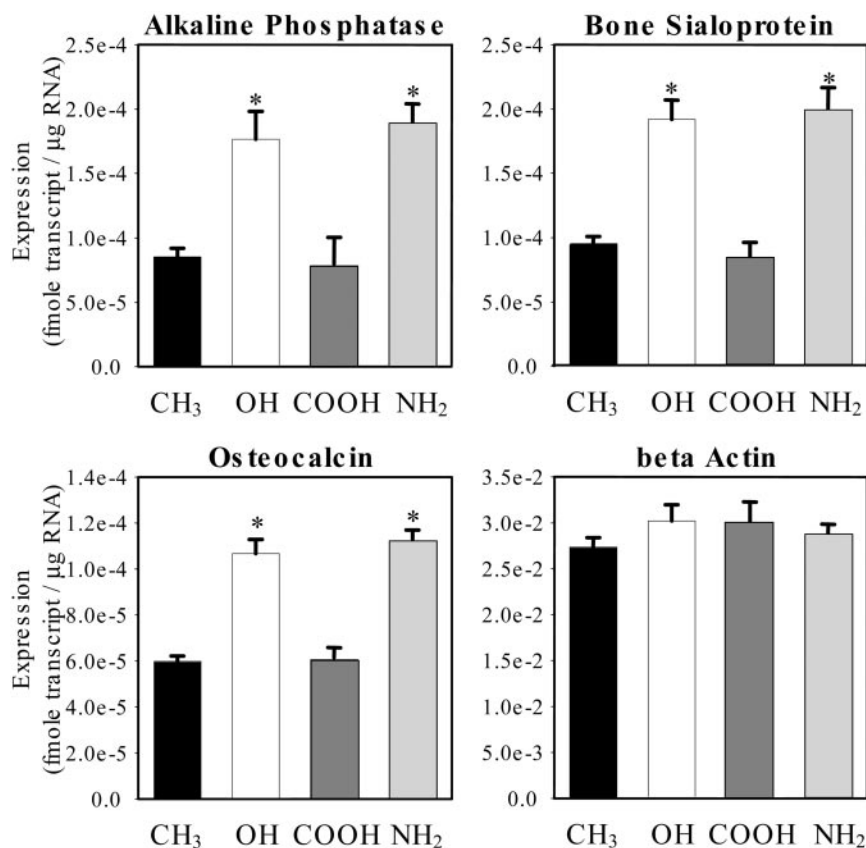


Fig. 2. Surface chemistry modulates osteoblastic gene expression. MC3T3-E1 cells were cultured on SAMs coated with equivalent FN surface densities (40 ng/cm²). Osteoblast-specific gene expression at 7 days was quantified by real-time RT-PCR (* vs. CH₃ and COOH, $P < 8 \times 10^{-6}$). Data are plotted as mean \pm SE.

dependent differences in gene expression on osteoblastic differentiation were further analyzed. In excellent agreement with gene expression results, ALP enzymatic activity was up-regulated on the OH and NH₂ surfaces compared with the COOH and CH₃ functionalities (Fig. 3A). Moreover, matrix mineralization displayed surface chemistry-dependent differences in a manner consistent with the patterns of osteoblast-specific gene expression and ALP enzymatic activity (Fig. 3B). Mineralization in these cultures occurs in scattered foci or “nodules,” which contain multiple layers of cells and associated extracellular matrix. The OH and NH₂ functionalities supported high levels of mineralized nodule formation, comparable to levels observed on FN-coated tissue culture polystyrene, whereas mineralization on the COOH and CH₃ surfaces was negligible. FTIR analyses demonstrated that the mineralized matrix deposited on the OH and NH₂ SAMs exhibits the chemical characteristics representative of a biological, carbonate-containing hydroxyapatite similar to the mineral phase of bone (Fig. 3C). In contrast, the matrix on the COOH and CH₃ surfaces did not display bands characteristic of a crystalline phosphate phase or carbonate content. Taken together, these results demonstrate that surface chemistry modulates osteoblast differentiation and matrix mineralization.

Integrin Binding Specificity for Adsorbed FN Regulates Surface Chemistry-Dependent Differentiation. The role of FN in surface chemistry-dependent osteoblast differentiation and mineralization was analyzed by using blocking antibodies. While SAMs were precoated with a fixed FN density (40 ng/cm²) to provide a single adhesive ligand, cells can reorganize this preadsorbed layer and deposit and/or incorporate other proteins that could influence

cellular activities. HFN7.1 monoclonal antibody was used to inhibit binding to the preadsorbed (human) FN. HFN7.1 blocks integrin binding to the central cell adhesive domain of FN, which contains the RGD binding motif (20). More importantly, this antibody is specific for human FN and does not cross-react with murine or bovine FN (21), allowing analysis of the role of preadsorbed (human) FN independently from secreted (murine) or serum-derived (bovine) FN. HFN7.1 and isotype control antibodies were added to 1-day cultures (to minimize disruption of initial adhesive events) and maintained throughout culture duration. No gross differences were observed in cell numbers among HFN7.1-treated and control cultures. Compared with controls, HFN7.1 completely blocked matrix mineralization on the OH and NH₂ SAMs, whereas the COOH and CH₃ remained devoid of mineralization (Fig. 4A). These results demonstrate that binding to the central cell adhesive domain of the preadsorbed FN controls the downstream effects of surface chemistry on osteoblast differentiation and mineralization. Commitment to differentiation in this system, as determined by matrix mineralization, occurred early in the process as addition of FN-blocking antibodies at either 1 or 4 days after cell seeding completely inhibited mineralization. Adding the blocking antibodies at 7 and 10 days reduced mineralization by 65% and 35%, respectively, compared with control cultures.

The up-regulated gene expression, ALP enzymatic activity, and matrix mineralization on the OH and NH₂ chemistries compared with the CH₃ surface correlate with the levels of bound $\alpha_5\beta_1$ integrin. To investigate the role of specific integrin receptors in surface chemistry-dependent mineralization, function-perturbing monoclonal antibodies directed against β_1 or β_3 integrin subunits and isotype controls were added to cultures at

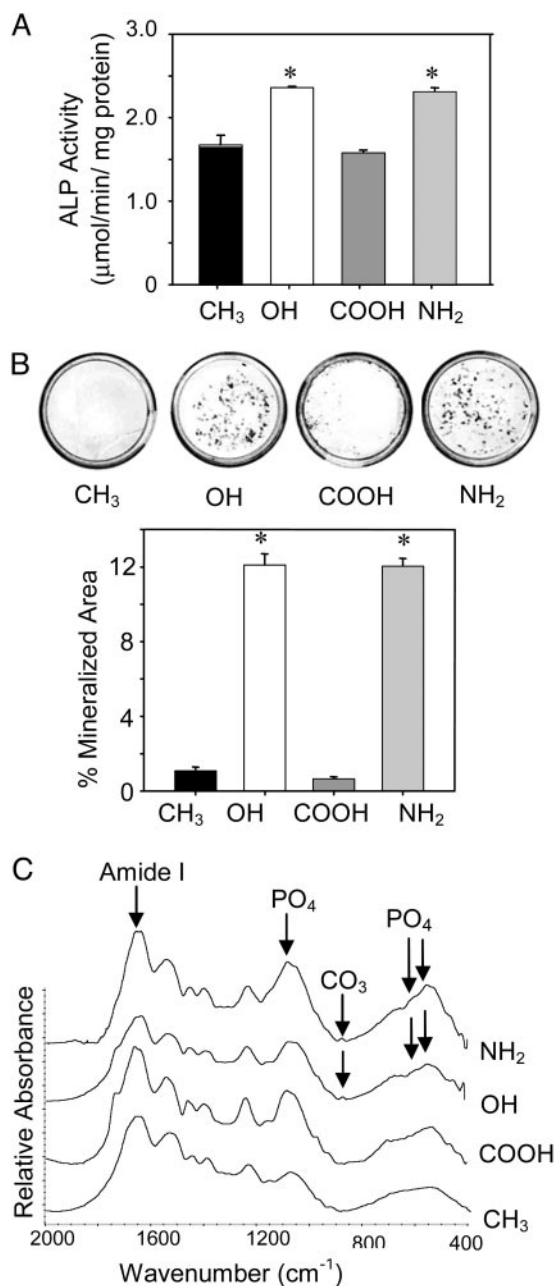


Fig. 3. Surface chemistry modulates ALP enzymatic activity and matrix mineralization. MC3T3-E1 cells were cultured on SAMs coated with equivalent FN surface densities (40 ng/cm²) and analyzed at 14 days. (A) ALP enzymatic activity exhibits surface chemistry-dependent differences. (B) von Kossa staining (Upper) for mineralized deposits (black) and quantification (Lower; mean \pm SE) showing differences among surface chemistries (* vs. CH₃ and COOH, $P < 0.01$). (C) FTIR spectra showing biological hydroxyapatite on OH and NH₂ SAMs. The doublet at 560 cm⁻¹/605 cm⁻¹ corresponds to crystalline phosphate phase representative of hydroxyapatite. The peak at 870 cm⁻¹ is assigned to carbonate substitution in hydroxyapatite phase. Peaks at 1,100 cm⁻¹ and 1,650 cm⁻¹ are assigned to phosphate and amide I (corresponding to protein) vibrations, respectively.

day 1 and maintained throughout the duration of culture. No adverse effects on cell adhesion or proliferation were evident for any antibody treatment. Equivalent levels of mineralization were observed between untreated (no antibody) and isotype control antibody-treated cultures. The β_1 -blocking antibody significantly inhibited mineralization on the OH and NH₂ surfaces to levels

corresponding to 20% and 50% of controls, respectively (Fig. 4B). The antibody against β_1 integrin also reduced mineralization on the COOH SAM relative to controls, but overall mineralization levels on this chemistry were significantly lower than those on the OH and NH₂ surfaces. Furthermore, antibody-treated cultures on OH and NH₂ surfaces recovered their mineralization ability when the antibody was removed from the culture media, indicating that the inhibitory effects of the antibody were reversible. Surprisingly, a β_3 -blocking antibody increased matrix mineralization on the NH₂ and COOH substrates (Fig. 4B). Notably, treatment with the β_3 -blocking antibody increased mineralization on the COOH surface by 400%, rescuing the block in mineralization on this surface to levels comparable to the OH and NH₂ substrates. As described previously, the COOH chemistry supports binding of $\alpha_5\beta_1$ to levels similar to the OH and NH₂ surfaces that support mineralization. In contrast to these surfaces, however, the COOH SAM also supports elevated levels of bound $\alpha_V\beta_3$. An explanation for the differences in differentiation among these surface chemistries is that binding of $\alpha_V\beta_3$ inhibits prodifferentiation signals triggered by $\alpha_5\beta_1$. This model is supported by the rescue in mineralization by the β_3 -blocking antibody on the COOH surface. Furthermore, the increase in mineralization by the β_3 -blocking antibody on the NH₂ SAM, but not the OH functionality, is also in agreement with this model because the NH₂ chemistry exhibits higher affinity for $\alpha_V\beta_3$ integrin than the OH SAM (14), albeit at levels significantly lower than the COOH surface. These results indicate that surface chemistry-dependent osteoblastic differentiation and matrix mineralization is regulated by integrin binding specificity ($\alpha_5\beta_1$ vs. $\alpha_V\beta_3$) for adsorbed FN.

Discussion

Using model biomaterial surfaces to present well defined chemistries, we demonstrate that surface chemistry modulates osteoblastic differentiation and matrix mineralization independently from alterations in cell proliferation. The OH and NH₂ surfaces up-regulate osteoblast-specific gene expression, ALP enzymatic activity, and matrix mineralization compared with the COOH and CH₃ substrates. Furthermore, these surface chemistry-dependent differences in cell differentiation are regulated by the binding of specific integrin receptors to adsorbed FN. Blocking antibodies against β_1 integrin inhibit matrix mineralization on the OH and NH₂ surfaces, whereas function-perturbing antibodies specific for β_3 integrin increase mineralization on the COOH SAM. Our observations for the contributions of specific integrins to osteoblast differentiation on these model biomaterials are in agreement with the roles of these receptors in osteoblast activities. Moursi *et al.* (22) showed that binding of integrin $\alpha_5\beta_1$ to FN is essential for osteoblast-specific gene expression and mineralization in primary osteoblast cultures. Moreover, overexpression of $\alpha_V\beta_3$ in MC3T3-E1 cells down-regulates osteoblastic differentiation and matrix mineralization (23).

We demonstrate that binding of specific integrin receptors on different biomaterial surfaces specifies downstream, higher-order cellular activities. Remarkably, integrin binding specificity is dictated by surface chemistry-induced changes in the structure of adsorbed FN. Integrins $\alpha_5\beta_1$ and $\alpha_V\beta_3$ bind to and compete for the RGD site on FN (24). Upon adsorption to these surfaces, FN undergoes changes in structure, including alterations in the central cell binding domain that modulate functional activity and integrin binding (13, 25). These surface chemistry-dependent structural changes differentially alter the affinity of specific integrins, resulting in shifts in integrin binding profiles. These differences in integrin binding profiles most likely regulate osteoblastic gene expression and mineralization via modulation of intracellular signaling pathways that regulate transcriptional activity. In fact, we previously showed that surface chemistry

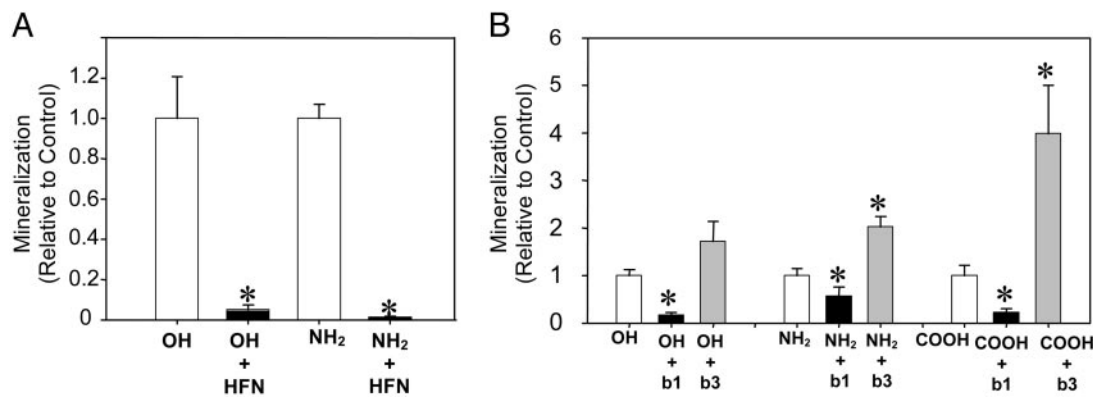


Fig. 4. Integrin binding specificity for adsorbed FN regulates the effects of surface chemistry on matrix mineralization. (A) Human FN-specific HFN7.1 antibody completely blocks mineralization on OH and NH₂ SAMs, demonstrating that binding to preadsorbed FN is critical for mineralization on these surfaces (mean \pm SE; * vs. control, $P < 0.01$). (B) Integrin-specific antibodies alter mineralization in a surface chemistry-dependent fashion. Antibodies against β_1 integrin block mineralization on OH and NH₂ SAMs, whereas anti- β_3 integrin antibodies up-regulate mineralization on COOH and, to a lesser extent, NH₂ (mean \pm SE; * vs. control, $P < 0.05$).

modulates focal adhesion assembly and site-specific focal adhesion kinase (FAK) phosphorylation (14). FAK plays a central role in integrating adhesion and growth factor signals to direct Runx2 transcriptional activity, osteoblast-specific gene expression, and matrix mineralization in this cell line (26, 27).

Our finding that integrin binding specificity regulates the effects of surface chemistry on osteoblast differentiation establishes a mechanism for the diversity of cellular responses to biomaterial surface properties. Furthermore, this mechanism could be exploited to engineer materials that control integrin binding specificity to elicit desired cellular activities. Current biomaterial strategies generally focus on preventing nonspecific protein adsorption and presenting short biomimetic motifs, such as RGD, to promote cell function (12, 28). However, short biomimetic motifs lack specificity among target receptors and exhibit limited biological activity when compared with the native biomolecule (29, 30). By engineering integrin specificity into

these hybrid materials and/or developing synthetic surfaces to control the functional presentation of adsorbed bioactive moieties, it may be possible to precisely control cell-material biomolecular interactions to activate specific signaling pathways and differentiation programs. These “bioengineered” materials could enhance integration of biomaterials and tissue-engineered constructs and improve the performance of biotechnological cell culture supports.

HFN7.1 antibody was obtained from the Developmental Studies Hybridoma Bank, which was developed under the auspices of the National Institute of Child Health and Human Development and is maintained by the University of Iowa, Department of Biological Sciences. This work was supported by the Whitaker Foundation and the Georgia Institute of Technology/Emory University National Science Foundation Engineering Research Council on the Engineering of Living Tissues (Grant EEC-9731643). B.G.K. was supported by a National Science Foundation Graduate Research Fellowship.

- García, A. J., Vega, M. D. & Boettiger, D. (1999) *Mol. Biol. Cell* **10**, 785–798.
- McClary, K. B., Ugarova, T. & Grainger, D. W. (2000) *J. Biomed. Mater. Res.* **50**, 428–439.
- Shen, M. & Horbett, T. A. (2001) *J. Biomed. Mater. Res.* **57**, 336–345.
- Allen, L. T., Fox, E. J., Blute, I., Kelly, Z. D., Rochev, Y., Keenan, A. K., Dawson, K. A. & Gallagher, W. M. (2003) *Proc. Natl. Acad. Sci. USA* **100**, 6331–6336.
- Gorbet, M. B. & Sefton, M. V. (2001) *J. Lab. Clin. Med.* **137**, 345–355.
- Brodbeck, W. G., Shive, M. S., Colton, E., Nakayama, Y., Matsuda, T. & Anderson, J. M. (2001) *J. Biomed. Mater. Res.* **55**, 661–668.
- Buser, D., Broggini, N., Wieland, M., Schenk, R. K., Denzer, A. J., Cochran, D. L., Hoffmann, B., Lussi, A. & Steinemann, S. G. (2004) *J. Dent. Res.* **83**, 529–533.
- Brodbeck, W. G., Patel, J., Voskerician, G., Christenson, E., Shive, M. S., Nakayama, Y., Matsuda, T., Ziats, N. P. & Anderson, J. M. (2003) *Proc. Natl. Acad. Sci. USA* **99**, 10287–10292.
- Anderson, J. M. (2001) *Annu. Rev. Mater. Res.* **31**, 81–110.
- Hench, L. L. & Polak, J. M. (2002) *Science* **295**, 1014–1017.
- Vreeland, W. N. & Barron, A. E. (2002) *Curr. Opin. Biotechnol.* **13**, 87–94.
- Hubbell, J. A. (2003) *Curr. Opin. Biotechnol.* **14**, 551–558.
- Keselowsky, B. G., Collard, D. M. & García, A. J. (2003) *J. Biomed. Mater. Res.* **66A**, 247–259.
- Keselowsky, B. G., Collard, D. M. & García, A. J. (2004) *Biomaterials* **25**, 5947–5954.
- Byers, B. A., Pavlath, G. K., Murphy, T. J., Karsenty, G. & García, A. J. (2002) *J. Bone Miner. Res.* **17**, 1931–1944.
- Sudo, H., Kodama, H. A., Amagai, Y., Yamamoto, S. & Kasai, S. (1983) *J. Cell Biol.* **96**, 191–198.
- Choi, J. Y., Lee, B. H., Song, K. B., Park, R. W., Kim, I. S., Sohn, K. Y., Jo, J. S. & Ryoo, H. M. (1996) *J. Cell. Biochem.* **61**, 609–618.
- Stephansson, S. N., Byers, B. A. & García, A. J. (2002) *Biomaterials* **23**, 2527–2534.
- Aubin, J. E. & Triffitt, J. T. (2002) in *Principles of Bone Biology*, eds. Bilezikian, J. P., Raisz, L. G. & Rodan, G. A. (Academic, San Diego), pp. 59–82.
- Bowditch, R. D., Halloran, C. E., Aota, S., Obara, M., Plow, E. F., Yamada, K. M. & Ginsberg, M. H. (1991) *J. Biol. Chem.* **266**, 23323–23328.
- Schoen, R. C., Bentley, K. L. & Klebe, R. J. (1982) *Hybridoma* **1**, 99–108.
- Moursi, A. M., Globus, R. K. & Damsky, C. H. (1997) *J. Cell Sci.* **110**, 2187–2196.
- Cheng, S. L., Lai, C. F., Blystone, S. D. & Avioli, L. V. (2001) *J. Bone Miner. Res.* **16**, 277–288.
- Danen, E. H., Aota, S., van Kraats, A. A., Yamada, K. M., Ruiters, D. J. & van Muijen, G. N. (1995) *J. Biol. Chem.* **270**, 21612–21618.
- Michael, K. E., Vernekar, V. N., Keselowsky, B. G., Meredith, J. C., Latour, R. A. & García, A. J. (2003) *Langmuir* **19**, 8033–8040.
- Tamura, Y., Takeuchi, Y., Suzawa, M., Fukumoto, S., Kato, M., Miyazono, K. & Fujita, T. (2001) *J. Bone Miner. Res.* **16**, 1772–1779.
- Xiao, G., Jiang, D., Thomas, P., Benson, M. D., Guan, K., Karsenty, G. & Franceschi, R. T. (2000) *J. Biol. Chem.* **275**, 4453–4459.
- Langer, R. & Tirrell, D. A. (2004) *Nature* **428**, 487–492.
- Pierschbacher, M., Hayman, E. G. & Ruoslahti, E. (1983) *Proc. Natl. Acad. Sci. USA* **80**, 1224–1227.
- García, A. J., Schwarzbauer, J. E. & Boettiger, D. (2002) *Biochemistry* **41**, 9063–9069.